J. Physiol. (1986), **381**, *pp.* 551–573
With 2 plates and 11 text-figures
Printed in Great Britain

ORGANIZATION OF SYNAPTIC TRANSMISSION IN THE MAMMALIAN SOLITARY COMPLEX, STUDIED *IN VITRO*

BY J. CHAMPAGNAT, MONIQUE DENAVIT-SAUBIÉ, KIRSTY GRANT AND K. F. SHEN*

From the Laboratoire de Physiologie Nerveuse, C.N.R.S., 91190 Gif-sur-Yvette, France

(*Received 2 January 1986*)

SUMMARY

1. Synaptic transmission and neuronal morphology were studied in the nucleus tractus solitarius and in the dorsal vagal motor nucleus (solitary complex), in coronal brain-stem slices of rat or cat, superfused *in vitro*.

2. Electrical stimulation of afferent fibres of the solitary tract evoked two different types of post-synaptic response recorded intracellularly in different solitary complex neurones. Labelling with horseradish peroxidase showed that these two sorts of orthodromically evoked responses were correlated with different post-synaptic neuronal morphologies.

3. The majority of recorded neurones ($n = 93$) showed a prolonged reduction in excitability following the initial solitary-tract-evoked excitatory post-synaptic potential (e.p.s.p.). A smaller number of neurones ($n = 53$) showed a prolonged increase in excitability following solitary tract stimulation. In no case did the solitary tract stimulation induce a burst of action potentials at high frequency.

4. The time-to-peak and the half-width of the initial solitary-tract-evoked e.p.s.p. were shorter in neurones with prolonged increased excitability than in those with prolonged reduced excitability. In neurones with prolonged reduced excitability, this e.p.s.p. was followed by a hyperpolarization lasting 60–100 ms. The latency of this inhibitory post-synaptic potential (i.p.s.p.) was 3–5 ms longer than that of the initial e.p.s.p. and its reversal potential was 10 mV more negative than the reversal potential of the response measured following application of γ-aminobutyric acid or glycine. In neurones with prolonged increased excitability, at a membrane potential of -40 to -50 mV, the initial solitary tract e.p.s.p. was followed by a prolonged depolarization lasting 100–400 ms.

5. Background synaptic activity was high in neurones with prolonged increased excitability, consisting of unitary e.p.s.p.s with an amplitude of more than 0·8 mV. This activity was increased for a period of 300–800 ms following solitary tract stimulation. Spontaneous excitatory potentials of more than 0·5 mV were not seen in neurones with prolonged reduced excitability. In these neurones, after intracellular injection of choride ions, reversed unitary i.p.s.p.s formed a background activity which was increased following stimulation of the solitary tract.

* Present address: Shanghai Brain Research Institute, 319 Yo-Yang Road, Shanghai, China.

6. Neurones with prolonged reduced excitability were found in the medial, ventral and ventrolateral part of the nucleus tractus solitarius and in the dorsal vagal motor nucleus where they were identified by their antidromic response to stimulation ventral and lateral to the tractus solitarius. In contrast, neurones with prolonged increased excitability were encountered frequently in the dorsomedial and commissural regions of the nucleus tractus solitarius.

7. Neurones with prolonged reduced excitability were of medium size with a dendritic arborization extending 200–300 μm from the soma. Neurones with prolonged increased excitability were small with a dendritic arborization restricted to a region not more than 100 μm from the cell body.

8. The existence of two different types of neurones in the solitary complex is discussed. It was found that the solitary tract nucleus *in vitro* contains the neuronal circuitry necessary for the generation of complex activity lasting several hundred milliseconds. It is proposed that neurones with prolonged reduced excitability integrate several different synaptic inputs. Neurones with prolonged increased excitability may be local interneurones which form the network responsible for the maintenance of long-lasting activity.

INTRODUCTION

Both anatomical and electrophysiological studies have established that the solitary complex including the different subnuclei of the nucleus tractus solitarius (n.t.s.) (Cajal, 1909; Kalia & Mesulam, 1980; Van der Kooy, Koda, McGinty, Gerfen & Bloom, 1984) and the dorsal vagal motor nucleus (d.v.m.n.), contain the terminal arborizations of visceral sensory fibres originating from vagal and glossopharyngeal nerves (Cajal, 1909; Kalia & Sullivan, 1982; Spyer, 1982). Reflex reactions involving visceral afferent inputs have been widely investigated (see Paintal, 1973). This has led to the concept that the n.t.s. is a key structure regulating cardiovascular (Kirchheim, 1976; Spyer, 1982) and digestive (Miller, 1982) functions. The d.v.m.n. is an output stage containing preganglionic neurones which have been functionally related to cardiovascular and digestive control (Jordan, Khalid, Schneiderman & Spyer, 1982; Shapiro & Miselis, 1985). In addition, the ventrolateral n.t.s. has been found in cats, to be essential in both reflex and central control of the respiratory rhythm (Von Euler, Hayward, Martilla & Wyman, 1973; Cohen, 1979; Richter, 1982; Morin-Surun, Champagnat, Boudinot & Denavit-Saubié, 1984; Davies, Kirkwood & Sears, 1985).

It is generally assumed that visceral afferent signals are transmitted through excitatory connexions with second-order sensory neurones located in the n.t.s. Electrical stimulation of visceral afferents has shown that evoked responses are mediated by a relay in the solitary complex.

However, little is known about the neuronal organization of the first sensory relay which takes place in the solitary complex.

In the n.t.s., short-term excitatory responses to single-shock electrical stimulation of visceral afferents have been observed, both *in vivo* (Gabriel & Seller, 1970; Von Euler *et al.* 1973; Berger & Averill, 1983; Backman, Anders, Ballantyne, Röhrig, Camerer, Mifflin, Jordan, Dickhaus, Spyer & Richter, 1984; Donoghue, Felder, Gilbey,

Jordan & Spyer, 1985) and *in vitro* (Champagnat, Siggins, Koda & Denavit-Saubié, 1985*b*; Miles, 1985), and found to be followed in many cases by a period of reduced excitability or inhibition. Synaptic potentials involved in this response and morphology of post-synaptic neurones are analysed in the present study. In addition, a second type of synaptic response is described: this consists of an initial excitation, followed by a period of increased excitability. Response types and synaptic mechanisms are correlated with neuronal localization and morphology, in the different subnuclei of the n.t.s. and in the d.v.m.n. This was done *in vitro* using coronal brain-stem slices from rat and from cat. In these preparations, the functional synaptic relationships between afferent inputs and solitary complex neurones are maintained, in an experimental situation in which the exogenous controls of their function are abolished (Champagnat, Denavit-Saubié & Siggins, 1983).

A preliminary report of this work has been presented (Champagnat, Grant, Shen & Denavit-Saubié, 1985*a*).

METHODS

Slice preparation

Experiments were performed on male Wistar rats (120–180 g) or 10 to 20-day-old kittens anaesthetized with ether and decapitated at the cervical spinal level. After a rapid craniotomy and removal of the forebrain, the spinal cord was cut and a brain-stem mass including the brain stem and the cerebellum was detached. The brain stem was separated from the cerebellum and transferred to a McIllwain tissue chopper. Throughout the procedure the exposed brain surfaces were continuously doused with a Krebs–Ringer solution previously refrigerated at 6 °C. Coronal slices 450 μm thick were sectioned from caudal to rostral. The three successive slices surrounding the obex were selected, transferred to a 70 μm thick, 0·5 mm^2 mesh nylon net support in the recording chamber.

Slice perfusion

The Krebs–Ringer solution contained (mM): NaCl, 124; KCl, 5; KH_2PO_4, 1·25; $MgSO_4 . 7\ H_2O$, 1·25; $CaCl_2$, 2; $NaHCO_3$, 26; glucose, 10; and was bubbled with a mixture of 95 % O_2 and 5 % CO_2. The perfusion system was gravity fed, allowing an incoming flow of 2–3 ml/min through a channel located below the level of the nylon net. The outflow was drained via the tip of a needle orientated horizontally 1 mm above the nylon net and connected to vacuum. The height of this needle determined the volume of solution in the chamber, i.e. 1·5 ml. A water bath surrounding the chamber was used to maintain the temperature thermostatically and to saturate the local atmosphere with warm, water-saturated, 95 % O_2, 5 % CO_2 mixture.

During the initial 15 min incubation period, the perfusion was interrupted and the fluid level in the chamber was lowered to expose the top surface of the slices to the local atmosphere ('interface'-type slice preparation), the temperature being maintained at 33 °C. Such incubation was found suitable to improve recovery, stability and viability of brain-stem slices. After this the fluid level was raised and the perfusion was started. This 'superfused'-type slice preparation was adopted for better and symmetrical diffusion of the fluids in the tissue. The temperature was kept constant ($\pm$0·1 °C) during the study of each neurone, and it was progressively increased up to 37 °C during the recording session. A similar proportion of neurones exhibited prolonged reduced or prolonged increased excitability (see Results) at 33–35 °C (i.e. during the first 5 h of experiments) and at 35–37 °C: therefore results are pooled in the present study.

Inhibitory amino acids γ-aminobutyric acid and glycine (Sigma) were dissolved in Krebs–Ringer solution (10^{-2} M, pH 7·4) and ejected under pressure (1 bar) from the tip of a micro-electrode positioned under visual control 0·2 mm away from the recording electrode. In some cases, magnesium chloride (up to 10 mM) or tetrodotoxin (1 μM) were added to the perfusion medium.

Anatomical observation of the solitary complex

Recording electrodes were positioned in the different subnuclei of the n.t.s. and in the d.v.m.n. or rats. Recordings in the kitten were restricted to the ventrolateral n.t.s. Anatomical subdivisions of the solitary complex were defined from our material stained with cresyl violet (Pls. 1 *B, D* and 2 *D*) in accordance with other studies performed in rats (Kalia & Sullivan, 1982; Van der Kooy *et al.* 1984) and cats (Kalia & Mesulam, 1980). A photographic atlas of the solitary complex was prepared from unstained 60 μm thick serial sections of the brain stem mounted in glycerine. In each experiment the position of recording and stimulating electrodes was noted using a binocular microscope (Wild Leitz) and recorded on the corresponding plane of the photographic atlas. Observations from different experiments were compared using, as land marks, the boundaries of the solitary complex with, dorsally, the gracilis nucleus, laterally, the tractus solitarius and, ventrally, the intercalatus or hypoglossal nucleus. The results are presented on a synthetic drawing (Fig. 2) of the solitary complex derived from the photographic atlas.

Stimulation procedure

Single stimuli of 0·05 ms were delivered from a programmable stimulator (Digitimer 3290) and applied using tungsten concentric bipolar electrodes (resistance, 0·5–1 MΩ). A stimulating electrode was positioned at the same precise site in all slices, on the dorsomedial part of the solitary tract (Fig. 2 *A* and *B*). This position was determined in preliminary experiments as follows. The tip of the stimulating electrode was placed at different positions while extracellular action potentials were recorded from solitary complex neurones. Similar experiments enabled the antidromic identification of neurones located in the d.v.m.n. using stimulating pulses delivered by a second bipolar electrode located outside the tractus solitarius, in a more ventrolateral position (Fig. 2 *C*).

When not stated otherwise, single stimuli were delivered at variable intervals of more than 5 s in order to avoid frequency depression of synaptic transmission.

Recording and staining techniques

Intracellular recordings were obtained with glass micropipettes filled with 3 M-potassium acetate (except in one experiment in which 3 M-potassium chloride was used) or with 4–10 % horseradish peroxidase (HRP, Sigma, type VI). HRP was dissolved in a 1 M-potassium acetate solution buffered with Tris at pH 8·6. The electrode was driven vertically in steps of 2–4 μm (AB Transvertex EM2). Membrane potential recordings and intracellular current injections were performed through the Wheatstone bridge of a d.c. pre-amplifier allowing capacity compensation. Voltage transients and injected currents were monitored and photographed from a storage oscilloscope (Tektronix, 5111) and displayed on an ink-pen recorder (Philips).

Intracellular ionophoresis of HRP was performed using depolarizing pulses of 0·6–2 nA and 0·7 s, repeated each second for 10–30 min. At least 1 h after injection, the slice was fixed for 1 h in buffered glutaraldehyde (4 %, pH 7·2) and then washed in phosphate buffer (pH 7·4) overnight. Slices were then embedded in agar (3 %) and sectioned serially in the coronal plane in an Oxford vibratome at 60 μm. HRP labelling was revealed using a modification of the Hanker–Yates technique (see Bell, Finger & Russell, 1981). Sections were counter-stained with cresyl violet and mounted in DPX (DePeX, Gurr). Morphological reconstructions were made from camera lucida drawings of serial sections.

Study of post-synaptic potentials

Neurones included in the present study showed an initial excitatory post-synaptic potential (e.p.s.p.) following tractus solitarius stimulation. Threshold voltage of stimulation was determined as giving rise to e.p.s.p.s of less than 0·5 mV. The amplitude of e.p.s.p.s reached maximal values of 5–25 mV when the voltage of stimulation was 2–3 times this threshold. Fluctuations in the shape of post-synaptic potentials (p.s.p.s) were used for analysis of compound synaptic potentials. Study of p.s.p.s was performed stimulating at a voltage of approximately 1·5 times the threshold, thus giving rise to submaximal p.s.p.s with an amplitude of 5 mV or less.

High gain d.c. recordings of p.s.p.s were made using a high frequency filter of 3 db, 10 KHz to reduce the background noise; a.c. recordings were avoided. The e.p.s.p wave form was described by the following shape parameters: time to peak, half-width, maximal rate of rise and maximal amplitude defined by others (Rall, Burke, Smith, Nelson & Frank, 1967). Synaptic potentials evoked at different membrane potentials were studied from the average of 10–50 digitized voltage

recordings. Membrane depolarization to a potential of −30 to −10 mV was achieved by intracellular current injection in the range of 1–2 nA: during this procedure, after a period of repetitive firing, the different components of the action potentials disappeared and the underlying p.s.p.s could be recorded. Averaging was performed using a PDP-8/E calculator operated on-line and displayed on the ink-pen recorder for detailed analysis.

Passive electrical properties of the neurones were evaluated in the linear portion of the current–voltage curve by injection of step hyperpolarizing currents of 0·1–0·4 nA. Input resistance was between 50 and 130 MΩ and membrane time constant was 5–10 ms. The Wheatstone bridge was balanced during extracellular recording before penetrations; its proper adjustment was again controlled after withdrawal of the electrode from the neurone. Membrane potentials were measured with respect to the 'zero' potential recorded after withdrawal of the electrode from the neurones.

RESULTS

The main body of the present study is based on intracellular recordings from 100 neurones of the solitary complex, with membrane potentials of −50 to −70 mV, overshooting action potentials, and response to orthodromic or antidromic stimulation. For comparison with previous *in vivo* studies, spontaneous and evoked firing of action potentials was studied in extracellular recordings from an additional fifty neurones.

Within this population of solitary complex neurones, two functional types were distinguished by their different responses to solitary tract stimulation. A first group of ninety-three neurones had a mean spontaneous firing frequency of 0·7 spikes/s and tractus solitarius stimulation evoked a single action potential (Fig. 1*A*). Repetition of the same stimulus showed that during a period of 40–400 ms following the first response, the excitability of the neurone was reduced since a second action potential could not be obtained. This type of response to solitary tract stimulation is defined in the present study as a prolonged reduced excitability (p.r.e.) following the initial, short-term excitatory response. Neurones showing this type of response were found in the n.t.s., particularly in the medial, ventral and ventrolateral n.t.s. and in the d.v.m.n. (Fig. 2*A*).

A second group of neurones, comprising about one-third of the total population ($n = 53$), was spontaneously active at a mean firing frequency of 3·2 spikes/s. Stimulation of the solitary tract evoked a first action potential followed by a period of increased excitability (p.i.e.) during which other action potentials occurred (Fig. 1*B*). Recordings performed in stable extracellular conditions indicate that up to seven action potentials (mean: 4·1) occur during the first 500 ms following the first orthodromic action potential. This excitatory response following stimulation of the solitary tract was never organized as a burst of repetitive action potentials; instead, in all cases, the frequency of action potentials decreased progressively to reach the control value of spontaneous firing. Neurones with this type of response were distributed more widely over the solitary complex than those described above (p.r.e.). P.i.e. neurones were encountered more frequently than p.r.e. neurones in the dorsomedial and commissural regions of the n.t.s. (Fig. 2*B*).

Both p.r.e. ($n = 13$) and p.i.e. ($n = 9$) types of response were found in the cat ventrolateral n.t.s. This proportion was similar in the rat ventrolateral n.t.s. in which eighteen neurones with p.r.e. and ten neurones with p.i.e. were recorded.

More than half of the d.v.m.n. neurones (twenty-one out of thirty-four tested)

identified by antidromic stimulation responded orthodromically by a single action potential to tractus solitarius stimulation (Figs. 2*A* and 3*Ba*). None of these d.v.m.n. neurones identified orthodromically showed the p.i.e. type of response to single tractus solitarius stimulation (Fig. 2*B*).

Antidromic action potentials observed in d.v.m.n. neurones were distinguished from those elicited orthodromically by the following criteria. At threshold stimulation for action potential generation, no underlying e.p.s.p. was observed (Fig. 3*Bb*); the

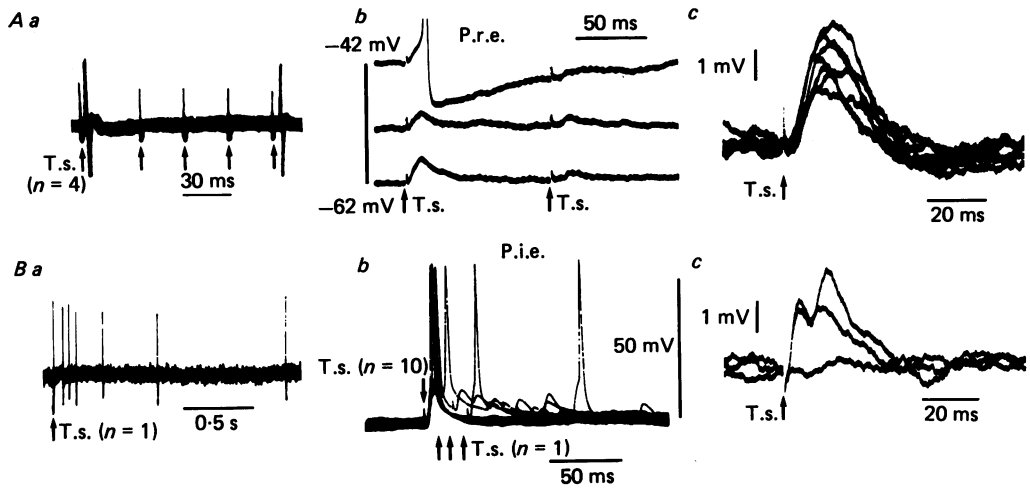

Fig. 1. *A*, synaptic effects of paired submaximal stimulation of the tractus solitarius (t.s.) in three neurones with prolonged reduced excitability (p.r.e.). All three neurones were recorded in the medial subnucleus of the tractus solitarius. *a*, four superimposed extracellular recordings comprising a conditioning stimulus (left) and a test stimulus 30, 60, 90 and 120 ms later. *b*, three traces superimposed at depolarized, resting and hyperpolarized membrane potentials. *c*, superimposed e.p.s.p. induced by a constant submaximal stimulation of the t.s. (the anatomical localization of this neurone is given in Fig. 8). *B*, synaptic effects of the stimulation of the t.s. in three neurones with prolonged increased excitability (p.i.e.). *a*, single sweep extracellular recording; neurone located in the ventrolateral nucleus tractus solitarius of kitten. *b*, ten superimposed traces showing conditioning stimulation of the t.s. ($n = 10$, downward arrow) followed, in three traces, by a single ($n = 1$) test stimulus of the t.s. (upward arrows) at a membrane potential of −55 mV (medial subnucleus of the t.s. of the rat). *c*, three superimposed traces following a constant submaximal stimulation of the t.s. The anatomical location of this neurone is illustrated by a triangle in Fig. 8 *Ab*.

initial segment/somato-dendritic inflexion was apparent on the rising phase of the antidromic action potential; antidromic spike generation followed repetitive stimulation at 500 Hz, but was blocked by a preceding orthodromic action potential evoked by depolarization of the soma (Fig. 4*Ba* and *b*). Furthermore, antidromic invasion continued to be observed 15 min after addition of 10 mM-magnesium ions to the perfusion medium, a procedure which was found to block synaptic transmission in the preparation. These criteria made it possible to distinguish synaptic responses from those elicited by antidromic stimulation of the recorded neurone.

After-hyperpolarizations (a.h.p.s) followed both orthodromic and antidromic

action potentials at resting or depolarized membrane potentials. During the a.h.p., the membrane resistance was reduced, as shown by the reduced amplitude and the faster time course of the voltage drop caused by intracellular current injection, when compared with similar current injection before the spike elicitation (Fig. 4*A*). The reversal potential of the a.h.p. following antidromic invasion was found to be 10–30 mV more negative than the resting potential and the estimated equilibrium potential for inhibitory post-synaptic potentials (i.p.s.p.s) (see below).

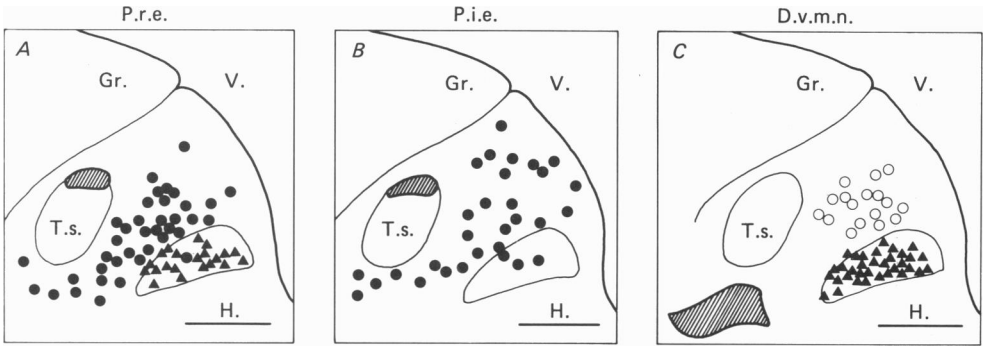

Fig. 2. Anatomical localization in the rat solitary complex of neurones identified by electrical stimulation. The solitary complex is presented by a synthetic drawing of the left dorsomedial medulla; the tractus solitarius and the dorsal vagal motor nucleus (d.v.m.n.) are outlined; gr., nucleus gracilis; h., hypoglossus nucleus; v., fourth ventricle; calibration: 250 μm. Hatched areas indicate the localization of the stimulating electrodes in the tractus solitarius (t.s., *A* and *B*) and in the ventrolateral area (*C*). Filled circles represent in *A* neurones with prolonged reduced excitability (p.r.e.), and in *B*, neurones with prolonged increased excitability (p.i.e.). Triangles represent neurones identified antidromically. Open circles in *C* localize neurones tested for and found insensitive to ventrolateral stimulation.

Neurones with p.i.e.

Background synaptic activity. Neurones with p.i.e. were characterized by a high background of synaptic activity (Fig. 5*A*). This was composed of depolarizing p.s.p.s, with a time to peak of 3–5 ms and a half-width of 7–13 ms. These p.s.p.s were studied at a membrane potential of −55 to −60 mV. The amplitude of individual e.p.s.p.s was an integer multiple of the smallest e.p.s.p.s observed. This unit e.p.s.p. which was constant in a given neurone had an amplitude of 0·8–1·5 mV. In the neurone illustrated in Fig. 5, 44 % of the e.p.s.p.s had an amplitude of 1·25 mV, 34 % had an amplitude of 2·5 mV, thus referred to as containing 2 units, and the remaining 22 % contained 3–7 units.

These large individual p.s.p.s were increased in amplitude by membrane hyperpolarization (Fig. 6*B*) but were still larger than 0·5 mV at a depolarized level of −50 or −40 mV (see Fig. 7*B* and *C*). At the same membrane potential, neurones with p.r.e. exhibited i.p.s.p.-like hyperpolarizations (see below) but no spontaneous individual e.p.s.p.s of more than 0·5 mV.

Fig. 5*C* illustrates the number of unit e.p.s.p.s as a function of time during the

period of increased excitability which follows stimulation of the tractus solitarius. Each individual e.p.s.p. was resolved into the number of unit p.s.p.s occurring at the same time. The background synaptic activity was thus found to be increased during a 300–800 ms period following tractus solitarius stimulation (see also Fig. 6*Ac*).

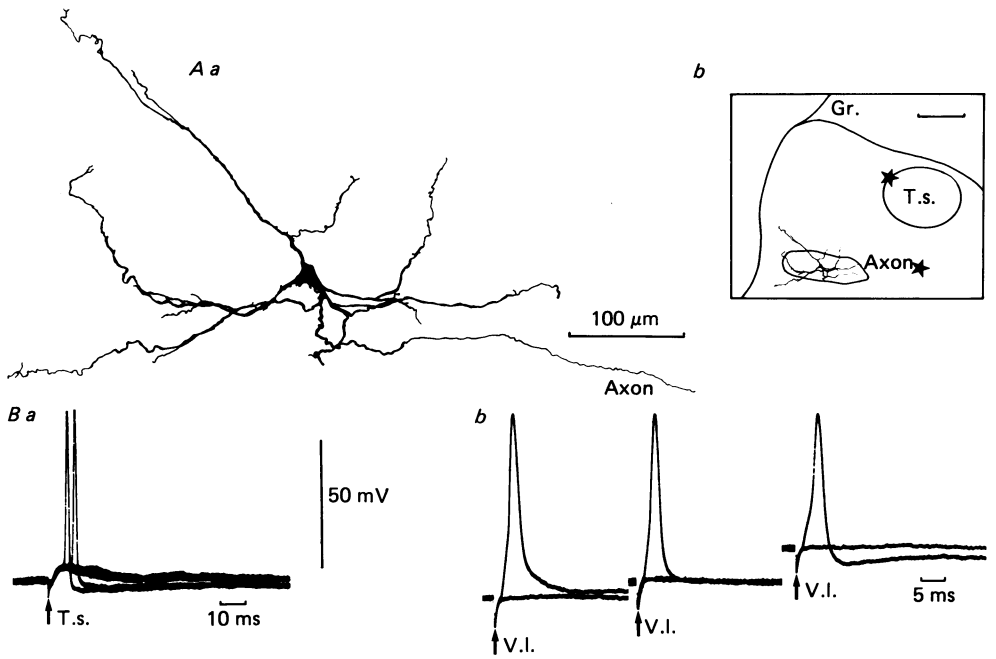

Fig. 3. *A*, morphology of a neurone with p.r.e. located in the d.v.m.n., reconstructed from four serial 60 μm thick sections. In this, as in following morphological Figures, the detailed morphology is presented (*a*) and the anatomical situation within the solitary complex is indicated in an inset (*b*); gr., nucleus gracilis; t.s., tractus solitarius; stars, localization of the stimulating electrodes; calibration in inset: 250 μm. *Ba*, orthodromic action potential and e.p.s.p. following stimulation of the t.s. (four superimposed sweeps), at the resting membrane potential (−60 mV). *Bb*, antidromic response of the same neurone after stimulation of the ventrolateral area of the n.t.s. (v.l.); the membrane potential was changed using current injections of −0·2, −0·1, and +0·1 nA; the bridge balance was under-compensated and in this Figure, the peak of action potentials was adjusted to the same level; in each recording, two traces corresponding to a stimulus just suprathreshold and another just subthreshold are superimposed.

Most p.s.p.s in neurones with p.i.e. remained subthreshold for spike generation at the resting membrane potential. The mean number of unit p.s.p.s evoked during the first 500 ms following the initial e.p.s.p. was compared with the mean number of action potentials recorded extracellularly during the same period. An average of 11·7 unit p.s.p.s were recorded intracellularly from neurones with p.i.e., compared with 4·1 action potentials which were recorded extracellularly from neurones with p.i.e. It is probable that several different presynaptic neurones with p.i.e. converge on the same post-synaptic neurone with p.i.e.

Synaptic responses to stimulation of the solitary tract. In addition to the increase of

background synaptic activity, stimulation of the tractus solitarius in neurones with p.i.e. evoked two synaptic potentials with different time courses: an initial e.p.s.p. and a prolonged depolarization. The shape parameters of the initial e.p.s.p., measured with stimulus intensity adjusted to give an e.p.s.p. of 4–5 mV, gave a time to peak of 2·5–4 ms (mean ± SD: 3·4 ± 0·9) i.e. 0·5–0·8 (0·6 ± 0·2) times the membrane

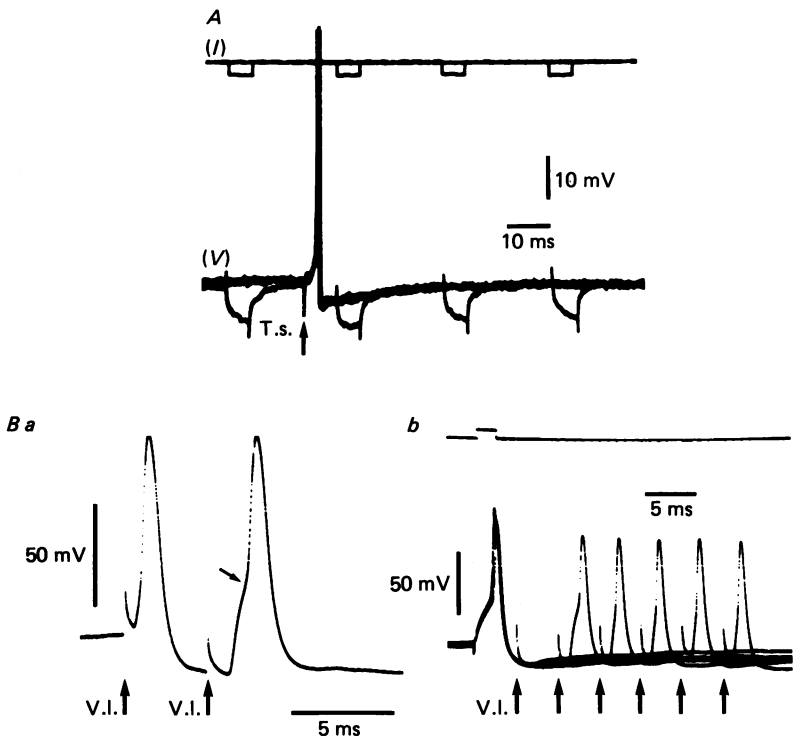

Fig. 4. Orthodromic (*A*) and antidromic (*B*) action potentials in neurones of the solitary complex *in vitro*. *A*, action potential evoked in a neurone with p.r.e. recorded with an electrode containing potassium acetate from the medial n.t.s. of rat: four traces are superimposed, each indicating the voltage drop (lower trace, *V*) resulting from one intracellular −0·1 nA, 5 ms current injection (upper trace, *I*). *B*, neurone with p.r.e. located in the d.v.m.n. of the rat. *a*, two stimulating pulses are delivered to the ventrolateral area of the n.t.s.; arrow indicates the initial segment/somato-dendritic inflexion of the antidromic action potential. *b*, six superimposed traces illustrate an action potential evoked by intracellular current injection of +0·1 nA and followed by a single antidromic stimulus 5–25 ms later.

time constant, a half-width of 7–15 ms (11·0 ± 3·0) i.e. 1·5–2·3 (1·8 ± 0·4) times the membrane time constant and a time constant of repolarization (e.g. see Fig. 5*B*) in the same range as the passive time constant of the membrane. These shape parameters were significantly different from those measured in neurones with p.r.e., indicating a faster time course for e.p.s.p.s in neurones with p.i.e. (see below and Fig. 1*Bc*). The time course of this initial e.p.s.p. was complicated by superimposed individual p.s.p.s similar to those forming the background synaptic activity (Figs. 1*Bb*, *c* and 5*B*). The initial e.p.s.p. decreased in amplitude during membrane

depolarization and an apparent equilibrium potential was extrapolated to between −20 and 0 mV (Fig. 7*A*).

The initial tractus-solitarius-evoked e.p.s.p. in neurones with p.i.e. was not followed by an i.p.s.p. This was demonstrated by recording synaptic potentials while depolarizing the membrane potential. A prolonged wave of depolarization was observed at membrane potentials between −50 and −40 mV (Fig. 7*B* and *C*). This

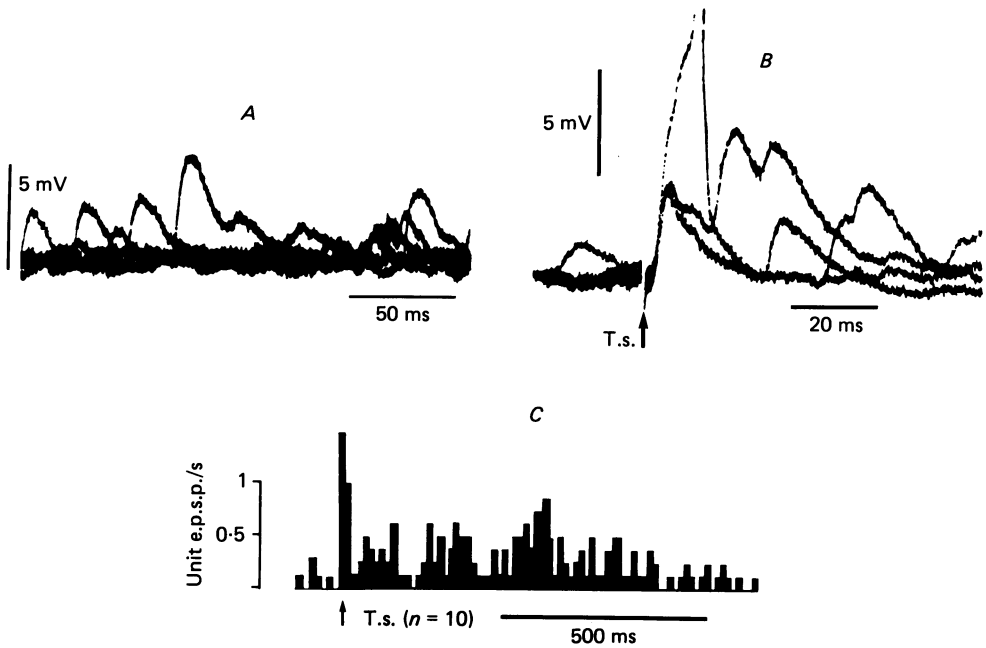

Fig. 5. Background synaptic activity in a neurone with p.i.e. located in the rat medial subnucleus of the n.t.s. and recorded with an electrode containing potassium acetate; membrane potential: −60 mV. *A*, six superimposed recordings of the membrane potential in the absence of electrical stimulation. *B*, four superimposed recordings during stimulation of the tractus solitarius (t.s.); in one trace an orthodromic action potential (truncated) is evoked. *C*, peristimulus time histogram showing the mean number of unit e.p.s.p.s (see text) following stimulation of the t.s. and averaged from ten recordings. Ordinate: number of unit e.p.s.p.s/s; abscissa: time following the stimulus; bin width: 10 ms.

depolarization appeared as a hump on the repolarization of the initial e.p.s.p. Its maximum amplitude was reached 100 ms after stimulation and repolarization to control potential 100–400 ms after stimulation: the time course of this wave was therefore 5–10 times slower than that of the initial e.p.s.p. The short-lasting e.p.s.p. and the long-term depolarization behaved differently with respect to membrane polarization: prolonged depolarization was missing at more hyperpolarized membrane potentials (−60 to −90 mV), at which large initial e.p.s.p.s are recorded. Both early and prolonged responses were abolished in the presence of extracellular magnesium ions (10 mM, two neurones) or tetrodotoxin (1 μM, one neurone) and must therefore depend on synaptic mechanisms.

Morphology of neurones with p.i.e. Intracellular staining with HRP was less

successful for neurones showing the p.i.e. type of response to tractus solitarius stimulation. Leakage of intracellular material probably occurred when the microelectrode was withdrawn and this resulted in a halo of HRP staining surrounding the recorded neurone (Pl. 2*D*) in many cases.

Most neurones of the p.i.e. type were small, with a soma diameter of 10–15 μm (Fig. 6*A*, Pl. 2*C*). Two to eight thin neurites, with a diameter of 1–2 μm, extended less than 100 μm from the cell body, but branched profusely within this area, ending in

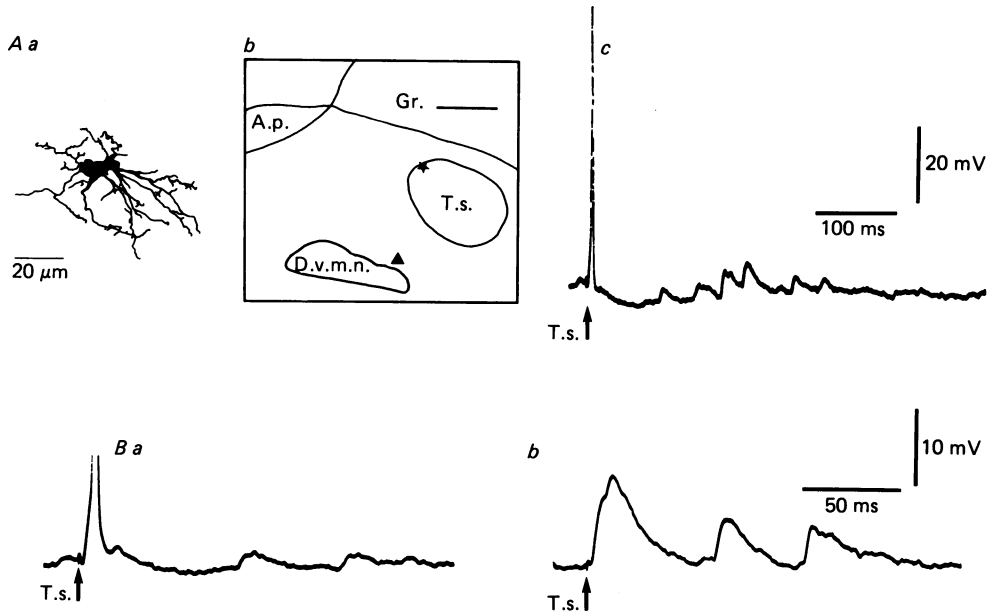

Fig. 6. Morphology and synaptic responses of a neurone with p.i.e. located in the rat ventral subnucleus of the n.t.s., reconstructed within a single 60 μm thick section. A.p., area postrema; d.v.m.n., dorsal vagal motor nucleus; g.r., gracilis nucleus; t.s., tractus solitarius; calibration in the inset: 250 μm. *c*, effect of the stimulation of the t.s. at a membrane potential of −65 mV. Recordings obtained at depolarized (−50 mV) and hyperpolarized (−90 mV) membrane potentials are illustrated in *Ba* and *Bb*, respectively.

clusters of short beaded filaments (Pl. 2*C*). Larger dendrites were not observed and the axon of these neurones could not be identified. A second type of morphology for neurones showing p.i.e. was observed in the dorsomedial n.t.s.; these had a small, elongated cell body, giving rise to two apically situated dendritic trunks. These dendrites showed little branching but stretched for some distance over the medial n.t.s., in the medio-lateral plane. Although this morphology appears different from that of the other type of p.i.e. neurone described above, no distinction could be made between these two types of neurone, based on recording of their intracellular activity.

Neurones with p.r.e.

Post-synaptic potentials evoked by stimulation of the solitary tract. In most neurones with p.r.e., submaximal stimulation of the solitary tract evoked an e.p.s.p.–i.p.s.p. sequence. Figs. 1*Ac* and 9 illustrate records from two morphologically identified

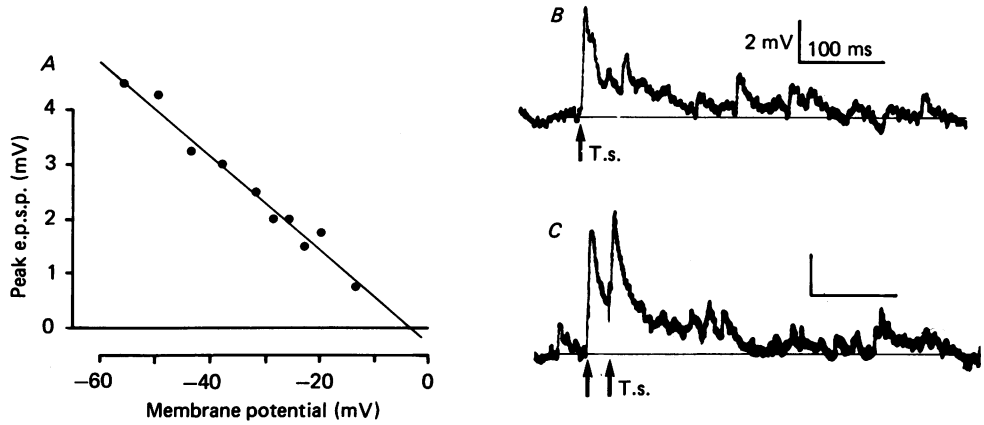

Fig. 7. *A*, plot of the peak amplitude of the early e.p.s.p. induced by stimulation of the tractus solitarius in a neurone with p.i.e. as a function of the membrane potential. *B* and *C*, slow p.s.p.s in neurones with p.i.e. *B*, single tractus solitarius (t.s.) stimulus; membrane potential: −50 mV; cat ventrolateral subnucleus of the t.s. *C*, paired t.s. stimuli; membrane potential: −40 mV; rat medial subnucleus of the t.s.; same calibration as *B*. Note the prolonged depolarization above the control membrane potential indicated by an horizontal line.

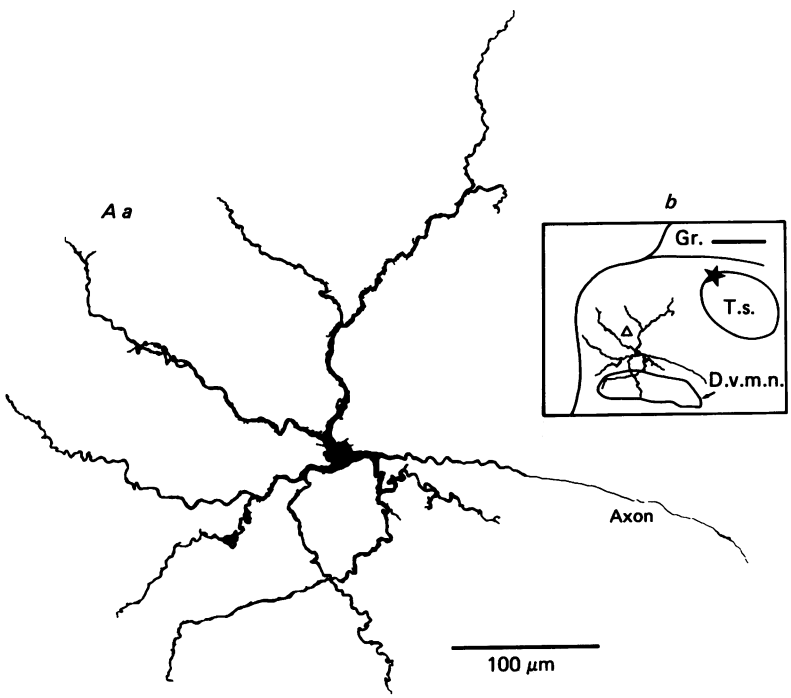

Fig. 8. Rat brain-stem slice: morphology of a neurone with p.r.e. located in the medial n.t.s., reconstructed from three serial 60 μm thick sections. D.v.m.n., dorsal vagal motor nucleus; gr., gracilis nucleus; t.s., tractus solitarius; star, localization of stimulating electrode; calibration in the inset: 250 μm. The e.p.s.p. of this neurone is illustrated in Fig. 1*Ac*. Triangle, location of a neurone with p.i.e., found in the same slice preparation and identified by its synaptic response (illustrated in Fig. 1*Bc*).

neurones from rat (Fig. 8) and cat (Fig. 9) n.t.s. respectively. Records from the two preparations were very similar, showing an initial e.p.s.p. of several millivolts which is followed by an i.p.s.p.-like hyperpolarization of about 1 mV, lasting more than 60 ms. In other cases, such as the neurone illustrated in Fig. 3, no i.p.s.p was found following the initial e.p.s.p.

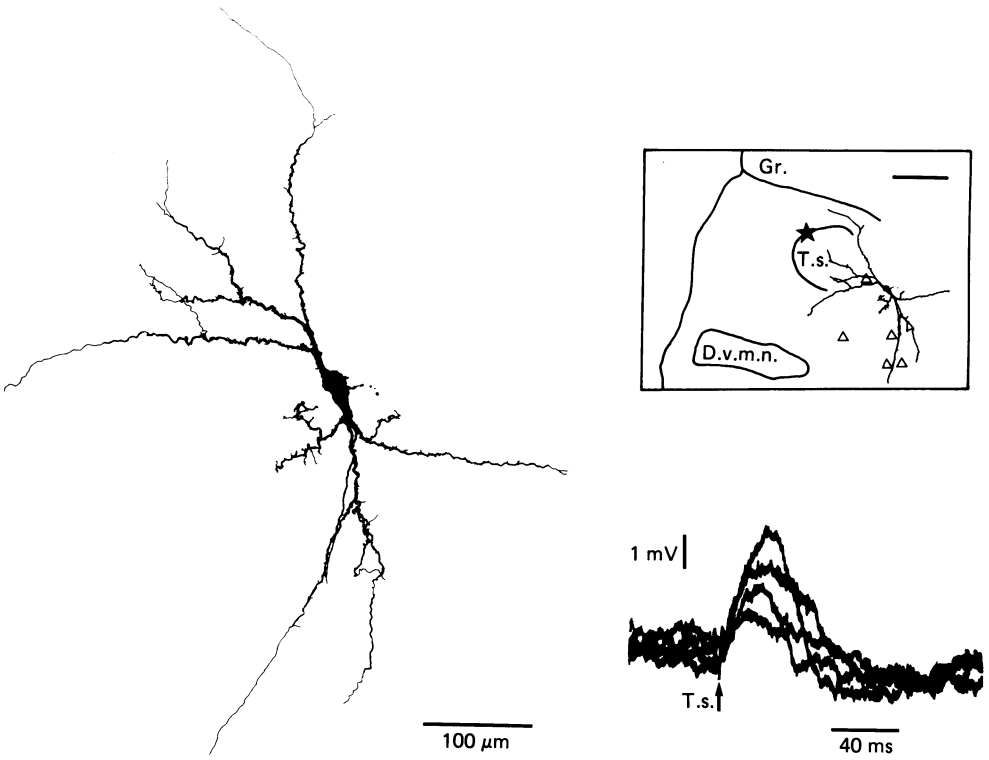

Fig. 9. Cat brain-stem slice: morphology and synaptic response of a neurone with p.r.e. located in the ventrolateral subnucleus of the n.t.s., reconstructed from four serial 60 μm thick sections. Calibration in the inset: 250 μm; d.v.m.n., dorsal vagal motor nucleus; gr., nucleus gracilis; t.s., tractus solitarius. Triangles in the inset indicate location of other neurones with soma diameter larger than 30 μm and identified by the cresyl violet counter-stain of the same slice. See Berger *et al.* (1984) for comparison with respiration-related neurones *in vivo*.

Measured from intracellular recordings of twenty-five neurones, the shape parameters of the tractus-solitarius-evoked e.p.s.p. were the following: time to peak, 5–30 ms (mean $\pm$ S.D.: 9·6 $\pm$ 5·1) i.e. 1–2·5 times (1·5 $\pm$ 0·7) the membrane time constant; half-width, 10–50 ms (23·6 $\pm$ 13·0) i.e. 2–5 times (3·4 $\pm$ 1·3) the membrane time constant. These shape parameters were significantly different from those measured in neurones with p.i.e., indicating a slower time course for e.p.s.p.s in neurones with p.r.e. (see Fig. 1 *Ac* and *Bc*). This difference was found significant at $P < 0{\cdot}0001$ using the Student's t test.

Hyperpolarization of the impaled cell up to 120 mV, by passage of current via the

micro-electrode, increased the amplitude of tractus-solitarius-evoked e.p.s.p.s. Similarly, depolarization of the cell membrane reduced e.p.s.p. amplitude and the apparent equilibrium potential of the e.p.s.p. was found to be between 0 and −20 mV in neurones with p.r.e. where no i.p.s.p. was demonstrated (Fig. 10*C*).

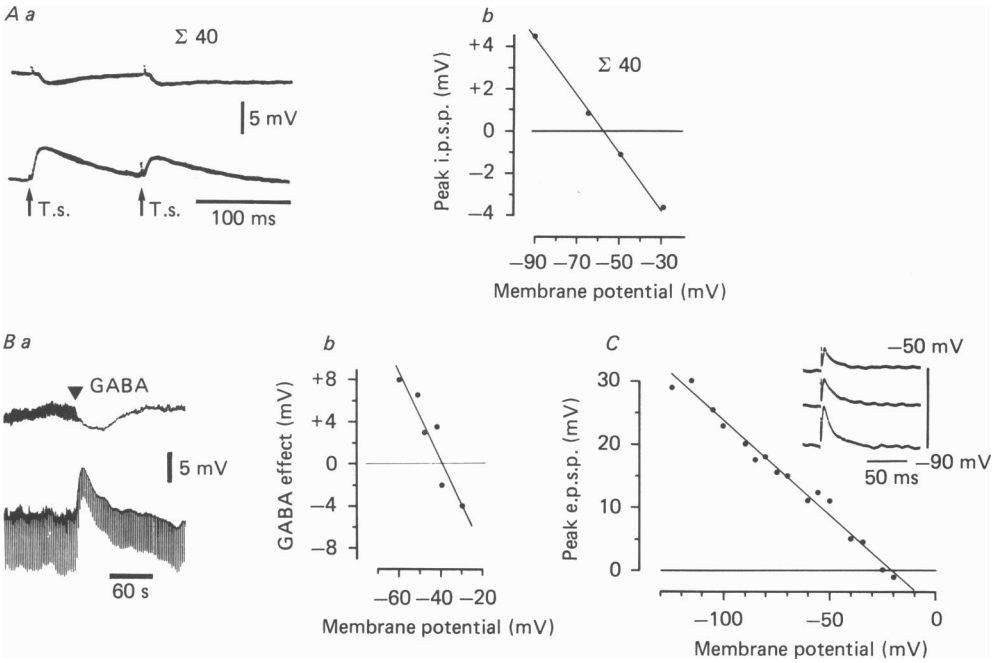

Fig. 10. Synaptic responses of neurones with p.r.e. at different membrane potentials. *A*, e.p.s.p.–i.p.s.p. sequence; *a*, average of forty recordings performed at a membrane potential of −50 and −90 mV during paired stimulation of the tractus solitarius (t.s.) separated by 100 ms. *b*, the amplitude of the p.s.p. was measured at the peak of i.p.s.p. and presented with a regression line as a function of the membrane potential. *Ba*, effect of pressure application of γ-aminobutyric acid (GABA, triangle) at −30 and −50 mV; in the lower trace the input resistance is monitored using intracellular injection of −0·2 nA, 500 ms square current pulses causing downward deflexions of the voltage recording. *b*, GABA effect is plotted as a function of the membrane potential; same neurone as in *A*, from the medial subnucleus of the t.s. *C*, e.p.s.p. in a different neurone with p.r.e., but lacking i.p.s.p.: plot of the amplitude of e.p.s.p. as a function of membrane potential. Regression line is drawn. Inset: e.p.s.p.s at different membrane potentials between −50 and −90 mV.

Large individual spontaneous p.s.p.s of more than 0·5 mV, such as those recorded in neurones with p.i.e., were not seen in neurones with p.r.e. recorded with electrodes containing potassium acetate. Variations of the e.p.s.p. wave form induced by a constant submaximal stimulus further indicate that large unitary e.p.s.p.s do not contribute to the early synaptic response of neurones with p.r.e. (Figs. 1*Ac* and 9).

Membrane depolarization was used to demonstrate i.p.s.p.s. These were prominent at −40 mV (Fig. 10*A*) and a delay of 3–5 ms was measurable between the onset of the i.p.s.p. and the end of the preceding e.p.s.p. whose amplitude was reduced at this

depolarized membrane potential. Between −50 and −60 mV mixed e.p.s.p.s and i.p.s.p.s were recorded, but at membrane potentials more negative than −60 mV, i.p.s.p.s were no longer observed. This i.p.s.p. was compared with the potential induced by the application of γ-aminobutyric acid and of glycine. γ-Aminobutyric acid or glycine induce hyperpolarization, which has been shown to be associated with an increased membrane conductance and to be reversed in these neurones at membrane potentials of −50 to −40 mV (Fig. 10*B*). This value is approximately 10 mV more positive than the observed inversion potential for tractus-solitarius-evoked i.p.s.p.s.

Effect of intracellular chloride ions and repetitive stimulation of the solitary tract. The consequences of the injection of chloride ions inside the neurones were investigated by recording of neurones with p.r.e. using intracellular electrodes containing potassium chloride. Within 10–60 min, a background activity of large (1–10 mV) spontaneous synaptic potentials developed. Since such large p.s.p.s are not observed with electrodes filled with potassium acetate (see above), it is probable that they result from reversal of individual chloride-dependent i.p.s.p.s. Stimulations were then delivered in the tractus solitarius and gave rise to an increased background activity similar to that observed in neurones with p.i.e. (using electrodes containing potassium acetate, see above).

These observations were clearer when the tractus solitarius was stimulated repetitively at a frequency of 5–50 Hz for 100–400 ms. The background activity of reversed i.p.s.p.s was increased for several seconds following stimulation. Several action potentials could be evoked by the stimulus and the response was therefore similar to that evoked by single stimuli in neurones with p.i.e.

Chloride-dependent post-synaptic inhibitory potentials are therefore a prominent feature of neurones with p.r.e.: they may explain most of the electrophysiological differences which were found between neurones with p.r.e. and p.i.e. and which were abolished following reversal of i.p.s.p.s.

Morphology of neurones with p.r.e. Twelve neurones with the p.r.e. type of response to tractus solitarius stimulation were reconstructed histologically following intracellular labelling with HRP. These showed a large variety in the shape of soma and the geometry of dendritic arborizations, although some common properties could be discerned. Reconstruction of these neurones from serial sections of the slice showed that the dendritic aborizations were intact and were contained within the slice. No severely truncated neurones were found and this suggests that for large neurones, the population sampled may depend on slice thickness and orientation.

In the rat solitary complex, cell bodies were spherical (Figs. 8 and 11), triangular (Fig. 3), or elongated (Fig. 9, Pl. 1*A*) and of fairly large size, varying from about 20 μm in diameter to about 20 μm wide by 50 μm long.

Up to six large primary dendrites with a diameter of 4–7 μm arose from the soma of neurones with p.r.e. The dendritic arborizations of all neurones with p.r.e. spread over 200–400 μm from the soma, thus covering more than one of the subnuclei of the solitary complex. Overlapping of dendritic arborizations was observed between the medial and ventral n.t.s. and the d.v.m.n. (Figs. 3, 8 and 11), between the ventral and ventrolateral n.t.s. and between the dorsolateral and ventrolateral n.t.s. (Figs. 9 and 11). Spiny, beaded and filament-like processes were present in abundance,

on primary and secondary dendrites and on the cell body of all neurones of the p.r.e. type (Pls. 1 *E* and 2 *A* and *B*).

The axons of d.v.m.n. neurones were identified in most cases, generally arising from the base of a primary dendrite and running laterally across the d.v.m.n. towards the stimulation site from which antidromic activation was obtained (Fig. 3, Pl. 1 *A*). The diameter of these axons was small (less than 2 μm) and it is possible that they are not myelinated. This is also suggested by the presence of small spine-like and beaded collaterals which could be observed along the length of the axon (Pl. 1 *C*), particularly within the d.v.m.n., close to the soma of other d.v.m.n. neurones, but also within the reticular formation.

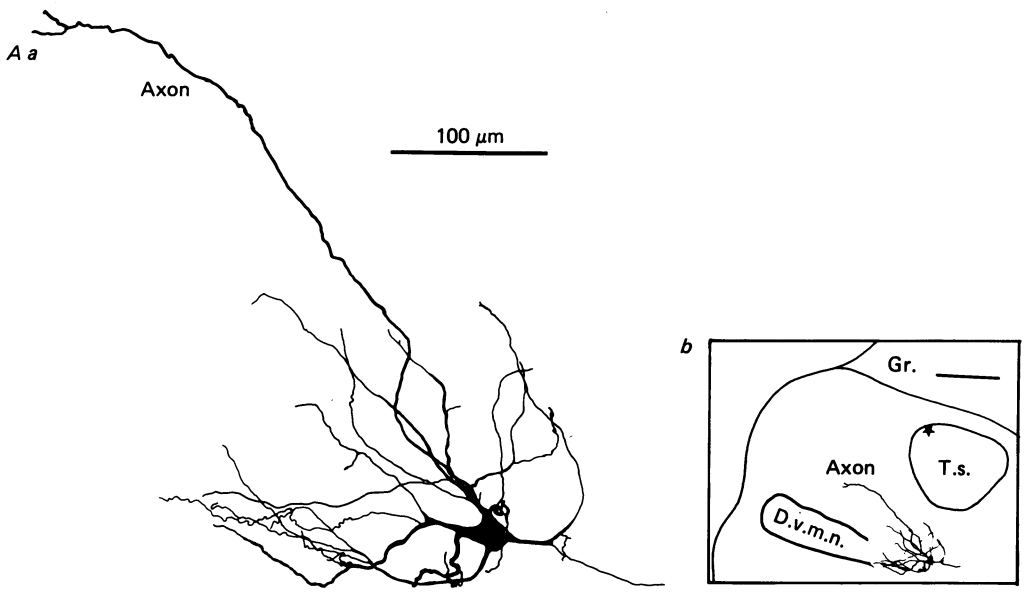

Fig. 11. *Aa–b*, morphology of a neurone with p.r.e. located in the rat ventral n.t.s., reconstructed from four serial 60 μm thick sections. D.v.m.n., dorsal vagal motor nucleus; gr., nucleus gracilis; t.s., tractus solitarius.

The axons of neurones of the subnuclei of the n.t.s. were less often identified. Axons running in the dorsal (not illustrated) or in the dorso-medial direction (Fig. 11), i.e. in a direction opposite to that of d.v.m.n. neurones, were observed in neurones of the rat ventral or ventrolateral subnucleus of the n.t.s. The neurone shown in Fig. 11 was situated lateral to the d.v.m.n. and ventral to the tractus solitarius. Its axon projected, without collaterals, in the dorso-medial direction. A terminal structure restricted to three beaded collaterals was found in the medial subnucleus of the n.t.s. In contrast, the neurone shown in Fig. 8, which was situated in the medial subnucleus of the n.t.s., sent its axon (Pl. 2 *A*) in a lateral direction, without branching, and the neurone of Fig. 9, located in the ventrolateral n.t.s. sent its axon in a ventral direction; these axons were lost before reaching a terminal structure.

DISCUSSION

These results demonstate that the coronal brain-stem slice *in vitro* contains the structures necessary for generation and maintenance of organized neuronal responses lasting for several hundred milliseconds in the solitary complex. Intracellular study of post-synaptic events in solitary complex neurones has confirmed that two types of neurone may be distinguished, based on their different synaptic responses to tractus solitarius stimulation. Intracellular labelling with HRP has revealed morphological differences which confirm this distinction of at least two major categories of neurone in the solitary complex.

Neurones with p.i.e.

Neurones with p.i.e. were characterized by a prominent background synaptic activity and by slow excitatory synaptic responses following stimulation of the tractus solitarius. Intracellular current injections were required to differentiate e.p.s.p.s from reversed i.p.s.p.s. This distinction is essential in the present study since i.p.s.p.s are absent in neurones with p.i.e.

The analysis of spontaneous post-synaptic activity indicates that groups of neurones with p.i.e. have excitatory interconnexions in the slice preparation. An incessant barrage of synaptic activity is not uncommon in brain slices (Johnston & Brown, 1984). Most of this activity disappears after blockade of sodium-dependent action potentials by extracellular tetrodotoxin and it must therefore represent nerve-impulse-dependent synaptic release within the local network preserved in the slice. In the solitary complex *in vitro*, propagation of activity within groups of neurones with p.i.e. leads to trains of individual p.s.p.s large enough to evoke post-synaptic action potentials, thus responsible for delayed changes of excitability in neurones with p.r.e. or p.i.e.

Neurones with p.i.e. are small and their structure is typical of local interneurones. Due to their small size and consequent difficulty in recording, it is probable that the number and importance of neurones classified as neurones with p.i.e. has been underestimated. Histologically studied neuropeptidergic neurones with a soma located in the solitary complex exhibit morphological features similar to the small neurones with p.i.e. labelled in the present study (Joseph, Pilcher & Bennett-Clarke, 1983; Higgins, Hoffman, Wray & Schwaber, 1984; Johansson, Hökfelt & Elde, 1984; Takagi, Kubota, Mori, Tateishi, Hamaoka & Tohyama, 1984). If it may be assumed, therefore, that most of these peptidergic neurones of the solitary complex are neurones with p.i.e., this would provide a neurobiological clue towards explaining the long-term control of visceral afferent information in the solitary complex.

Neurones with p.r.e.

Neurones with p.r.e. were characterized by the slow time course of their early e.p.s.p. in response to tractus solitarius stimulation, and by the i.p.s.p. and the continuing prolonged reduced excitability which followed.

Time course of the early e.p.s.p. Extracranially, the vagus and glossopharyngeal nerves contain sensory fibres with a wide range of diameters and conduction velocities (Paintal, 1973; Mei, Condamin & Boyer, 1980). In the slice preparation,

the conduction distance is very short, and thus temporal dispersion in the arrival of afferent impulses resulting from differences in conduction velocities is likely to be minimal and will not influence the time course of the early e.p.s.p.

Solitary complex neurones of the p.r.e. type have widely arborizing, spiny dendritic trees, and since it has been shown by several authors (Rall *et al.* 1967; Jack, Redman & Wong, 1981) that the time course of an e.p.s.p. is indicative of the electrotonic location of its synapses on the post-synaptic membrane, it may be supposed that the slow time course of the early e.p.s.p. is due to the integration of synaptic activity arriving with a wide spatial distribution on p.r.e. neurones, via several afferent fibres.

I.p.s.p. and p.r.e. The reversal of i.p.s.p.s occurred at potentials close to the resting potential and was modified following injection of chloride ions into the neurones. This observation suggests that chloride ions are involved in these potentials. The driving force of chloride ions was investigated by studying the effect of inhibitory amino acids, γ-aminobutyric acid and glycine (Curtis, Hösli, Johnston & Johnston, 1968; Krnjevic, Puil & Werman, 1977), taken as an index of chemically induced chloride current in solitary complex neurones. The present measurements indicate that the i.p.s.p.s consistently reversed at membrane potentials slightly more negative than the effect of inhibitory amino acids. This would suggest that chloride is not the only ionic species involved in i.p.s.p.s and that an additional increased permeability, probably to potassium ions, explains this difference. Alternatively, it is possible that inhibitory synapses are located in remote positions on the dendritic tree at sites not adequately voltage controlled by a somatic injection of d.c. current.

Functional importance of p.r.e. The presence of both e.p.s.p.s and i.p.s.p.s following tractus solitarius stimulation further shows that neurones with p.r.e. receive a variety of synaptic inputs. The recent demonstration of hyperpolarizing potentials following stimulation of the carotid sinus nerve *in vivo* emphasizes the functional importance of such inhibitory mechanisms in cardiovascular and respiratory control by the n.t.s. (Donoghue *et al.* 1985). In the present study, the delay between the onset of the monosynaptic e.p.s.p. and the following i.p.s.p. indicates that i.p.s.p.s. are generated by a polysynaptic pathway. Thus it is concluded that the *in vitro* slice preparation of the solitary complex contains inerneurones which are inhibitory to neurones with p.r.e. and that viscerally originating inhibitory effects are mediated by this pathway.

When paired, condition and test, stimuli were applied to the solitary tract, the amplitude of the 'test' e.p.s.p. was reduced both during the a.h.p. of the 'conditioning' action potential and for several hundred milliseconds following the return to the normal resting potential. While the former reduction is related to the increased membrane conductance during the spike a.h.p., it was observed that prolonged reduced excitability occurred even when the conditioning stimulus was insufficient to generate an action potential. This suggests that a presynaptic mechanism is involved (Champagnat *et al.* 1985*b*; Miles, 1985), possibly that of presynaptic inhibition of some visceral afferents by others via axo-axonic synapses existing in the n.t.s. (Chiba & Kato, 1978).

During natural autonomic reflexes *in vivo*, sensory afferents of several modalities converged on single neurones of the solitary complex (see Donoghue *et al.* 1985) and the shape of synaptic potentials may reflect distribution of synapses over the

post-synaptic somatodendritic membrane (Backman *et al.* 1984). In the present study stimulation in the solitary tract may have excited dendrites of the neurones under investigation. The time course of the p.s.p.s obtained is slower than that which would be expected from dendritically originating action potentials in these neurones (Champagnat, Jacquin & Richter, 1986). We therefore believe that dendritic contribution to the p.s.p.s is mainly of synaptic origin.

When electrically stimulating the tractus solitarius *in vitro*, it is not possible to distinguish between fibres of different peripheral origin. However, in the present study, the spike activity of neurones with p.r.e. is regulated by the integration of a variety of monosynaptic excitatory inputs, by local inhibitory interneurones and by inhibitory interaction at the level of incoming sensory information. Furthermore, the dendritic tree of neurones with p.r.e was found to extend over a wide area, covering several subnuclei of the solitary complex. Synaptic contacts with sensory afferents which spread over different parts of the solitary complex are therefore probable (Berger & Averill, 1983). It is therefore likely that neurones with p.r.e. accomplish an integrative function in the n.t.s.

Anatomo-functional identification of neurones with p.r.e.

While neurones with p.r.e were found throughout the solitary complex, certain functional groups may be identified by correlation of their morphology with data obtained *in vivo*.

D.v.m.n. Dorsal vagal neurones form one of these functional groups, located ventral to the n.t.s. Extracellular studies *in vivo* with antidromic identification have established the localization, in the dorsal vagal nucleus, of vagal efferent neurones with a cardiovascular or a digestive function (Jordan *et al.* 1982; Shapiro & Miselis, 1985). Although they are perhaps the most easily recordable cells in the rat solitary complex *in vitro*, their proper identification in this preparation requires either antidromic activation or HRP labelling, in order to avoid confusion with cells of the ventral subdivisions of the n.t.s. Morphologically, they resemble neurones described by Cajal (1909) as dorsal vagal motor neurones and shown using immunohistochemical techniques to be cholinergic (Armstrong, Clifford, Levey, Wainer & Terry, 1983) or monoaminergic (Ritchie, Westlund, Bowker, Coulter, & Leonard, 1982). Their axon trajectory follows the same course as that described by retrograde HRP labelling of the vagus nerve in rats (Kalia & Sullivan, 1982; McLean & Hopkins, 1982).

The present study demonstrates synaptic connexions between the tractus solitarius afferents and d.v.m.n. neurones and indicates that the entire reflex arc from the afferent fibres to the efferent neurones can be preserved in the slice preparation.

Dorsal respiratory neurones. It has been shown that neurones with a periodic discharge pattern related to the respiratory rhythm (see Cohen, 1979; Richter, 1982) are present in the cat ventral and ventro-lateral n.t.s. *in vivo*. In addition, inspiratory neurones, with a morphology similar to that of p.r.e. neurones illustrated here, have been described in the ventro-lateral n.t.s. in cats (Von Euler *et al.* 1973; Berger, Averill & Cameron, 1984). It is therefore probable that some of the p.r.e. neurones identified in the present *in vitro* study belong to these functional populations.

However, no evidence of bursting activity was observed in these neurones in the slice preparation, either in the rat or in the cat. Thus it is concluded that the

generation of rhythmic neuronal activity resembling that of respiratory neurones *in vivo* (Denavit-Saubié, Champagnat & Zieglgänsberger, 1978) requires the integrity of synaptic connexions between the solitary complex and the brain-stem network of respiratory neurones (Merrill, Lipski, Kubin & Fedorko, 1983).

Long-term control of neuronal activities in the solitary complex

The functional importance of long-term control of respiratory and cardiovascular parameters has been recognized, although the electrophysiological basis of these phenomena is unknown at the neuronal level. Prolonged changes of the respiratory rhythm induced by stimulation of chemoreceptor afferents have been reported and related to control mechanisms independent of the respiratory controller (Eldrige, Gill-Kumar & Millhorn, 1981). The present study raises the possibility that such long-term effects can be generated within the local network of solitary complex neurones which are preserved in the slice preparation. The present results demonstrate that prolonged changes of excitability in solitary complex neurones are related to increase in background synaptic activity generated by neurones with p.i.e.

In addition, generation of long-term post-synaptic effects within the solitary complex may involve the release of neurotransmitter substances with a prolonged post-synaptic action. This is a likely basis for the slow e.p.s.p.s recorded in neurones with p.i.e. following stimulation of the tractus solitarius. Slow e.p.s.p.s are characterized by their time course and by the fact that they were larger when the membrane was depolarized with respect to the resting membrane potential. This is in contrast with what was observed for i.p.s.p.s and for early e.p.s.p.s. A simple explanation would be that slow e.p.s.p.s in solitary complex neurones are mediated by a decrease in permeability to potassium ions, as described for instance in the spinal cord (Urban & Randic, 1984).

The absence of slow e.p.s.p.s at hyperpolarized membrane potentials also contrasts with the properties of low threshold calcium currents which participate in the generation of synaptically-induced bursts of action potentials in a variety of structures in a mammalian central nervous system (e.g. see Connors, Gutnick & Prince, 1982). Calcium currents are present in the solitary complex (Champagnat *et al.* 1986) although they do not generate a bursting pattern of activity. The different components of the action potentials observed occasionally in the present study may be tentatively related to such calcium currents. However, following tractus solitarius stimulation, no bursting pattern was observed, even after previous membrane hyperpolarization, and therefore calcium currents are likely play a minor role in the generation of prolonged excitatory responses described presently.

The present paper indicates that the neuronal organization of the first sensory relay which takes place in the solitary complex involves two types of neurones. These determine two types of transmission at this level: first, a short-term 'phasic' excitatory transmission which is subjected to inhibitory controls, and secondly, a long-term 'tonic' modulation of on-going activity.

This work was supported by an ATP of the Centre National pour la Recherche Scientifique and by the Fondation pour la Recherche Médicale. K. F. Shen was supported by the Institut National pour la Santé et la Recherche Médicale.

REFERENCES

ARMSTRONG, D. M., CLIFFORD, B. S., LEVEY, A. I., WAINER, B. H. & TERRY, R. D. (1983). Distribution of cholinergic neurons in rat brain: demonstrated by the immunocytochemical localization of choline acetyltransferase. *Journal of Comparative Neurology* **68**, 216–253.

BACKMAN, S. B., ANDERS, C., BALLANTYNE, D., RÖHRIG, N., CAMERER, H., MIFFLIN, S., JORDAN, D., DICKHAUS, H., SPYER, K. M. & RICHTER, D. W. (1984). Evidence for a monosynaptic connection between slowly adapting pulmonary stretch receptor afferents and inspiratory beta neurones. *Pflügers Archiv* **402**, 129–136.

BELL, C. C., FINGER, T. E. & RUSSELL, C. J. (1981). Central connections of the posterior lateral line lobe in mormyrid fish. *Experimental Brain Research* **42**, 9–22.

BERGER, A. J. & AVERILL, D. B. (1983). Projection of single pulmonary stretch receptors to solitary tract region. *Journal of Neurophysiology* **49**, 819–830.

BERGER, A. J., AVERILL, D. B. & CAMERON, W. E. (1984). Morphology of inspiratory neurons located in the ventrolateral nucleus of the tractus solitarius of the cat. *Journal of Comparative Neurology* **224**, 60–70.

CAJAL, S. R. Y. (1909). *Histologie du système nerveux de l'homme et des vertébrés*. Paris: Maloine.

CHAMPAGNAT, J., DENAVIT-SAUBIÉ, M. & SIGGINS, G. R. (1983). Rhythmic neuronal activities in the nucleus of the tractus solitarius isolated *in vitro*. *Brain Research* **280**, 155–159.

CHAMPAGNAT, J., GRANT, K., SHEN, K. F. & DENAVIT-SAUBIÉ, M. (1985*a*). Neuronal morphology and synaptic transmission in the solitary complex *in vitro*. In *Neurogenesis of Central Respiratory Rhythm*, ed. BIANCHI, A. L. & DENAVIT-SAUBIÉ, M., pp. 157–164. Lancaster: MTP Press.

CHAMPAGNAT, J., JACQUIN, T. & RICHTER, D. W. (1986). Voltage-dependent currents in neurones of the nuclei of the solitary tract of rat brainstem slices. *Pflügers Archiv* **406**, 372–379.

CHAMPAGNAT, J., SIGGINS, G. R., KODA, L. Y. & DENAVIT-SAUBIÉ, M. (1985*b*). Synaptic responses of neurons of the nucelus tractus solitarius. *Brain Research* **325**, 49–56.

CHIBA, T. & KATO, M. (1978). Synaptic structure and quantification of catecholaminergic axons in the nucleus tractus solitarius of the rat: possible modulatory roles of catecholamines. *Brain Research* **151**, 323–338.

COHEN, M. I. (1979). Neurogenesis of respiratory rhythm in the mammal. *Physiological Reviews* **59**, 1105–1173.

CONNORS, B. W., GUTNICK, M. J. & PRINCE, D. A. (1982). Electrophysiological properties of neocortical neurons *in vitro*. *Journal of Neurophysiology* **48**, 1302–1335.

CURTIS, D. R., HÖSLI, L., JOHNSTON, G. A. R. & JOHNSTON, I. H. (1968). The hyperpolarization of spinal motoneurones by glycine and related amino acids. *Experimental Brain Research* **5**, 235–258.

DAVIES, J. G. McF., KIRKWOOD, P. A. & SEARS, T. A. (1985). The detection of monosynaptic connexions from bulbospinal neurones to inspiratory motoneurones in the cat. *Journal of Physiology* **386**, 33–62.

DENAVIT-SAUBIÉ, M., CHAMPAGNAT, J. & ZIEGLGÄNSBERGER, W. (1978). Effects of opiates and methionine-enkephalin on pontine and bulbar neurones of the cat. *Brain Research* **155**, 55–67.

DONOGHUE, S., FELDER, R. B., GILBEY, M. P., JORDAN, D. & SPYER, K. M. (1985). Post-synaptic activity evoked in the nucleus tractus solitarius by carotid sinus and aortic nerve afferents in the cat. *Journal of Physiology* **360**, 261–273.

ELDRIDGE, F. L., GILL-KUMAR, P. & MILLHORN, D. E. (1981). Input–output relationships of central neural circuits involved in respiration in cats. *Journal of Physiology* **311**, 81–95.

GABRIEL, M. & SELLER, H. (1970). Interaction of baroreceptor afferents from carotid sinus and aorta at the nucleus tractus solitari. *Pflügers Archiv.* **318**, 7–20.

HIGGINS, G. A., HOFFMAN, G. E., WRAY, S. & SCHWABER, J. S. (1984). Distribution of neurontensin-immunoreactivity within baroreceptive portions of the nucleus of the tractus solitarius and the dorsal vagal nucleus of the rat. *Journal of Comparative Neurology* **226**, 155–164.

JACK, J. J. B., REDMAN, S. J. & WONG, K. (1981). The components of synaptic potentials evoked in cat spinal motoneurones by impulses in single group Ia afferents. *Journal of Physiology* **321**, 65–96.

JOHANSSON, O., HÖKFELT, T. & ELDE, R. P. (1984). Immunohistochemical distribution of somatostatin-like immunoreactivity in the central nervous system of the adult rat. *Neuroscience* **13**, 265–339.

JOHNSTON, D. & BROWN, T. H. (1984). Biophysics and microphysiology of synaptic transmission in hippocampus. In *Brain Slices*, ed. DINGLEDINE, R., pp. 51–86. New York and London: Plenum Press.

JORDAN, D., KHALID, M. E. M., SCHNEIDERMAN, N. & SPYER, K. M. (1982). The location and properties of preganglionic vagal cardiomotor neurones in the rabbit. *Pflügers Archiv* **395**, 244–250.

JOSEPH, S. A., PILCHER, W. H. & BENNETT-CLARKE, C. (1983). Immunocytochemical localization of ACTH perikarya in nucleus tractus solitarius: evidence for a second opiocortin neuronal system. *Neuroscience Letters* **38**, 221–225.

KALIA, M. & MESULAM, M. M. (1980). Brainstem projections of sensory and motor components of the vagus complex in the cat. II. Laryngeal, tracheobronchial, cardiac and gastrointestinal branches. *Journal of Comparative Neurology* **193**, 467–508.

KALIA, M. & SULLIVAN, J. M. (1982). Brainstem projections of sensory and motor components of the vagus nerve in the rat. *Journal of Comparative Neurology* **211**, 258–264.

KIRCHHEIM, H. R. (1976). Systemic arterial baroreceptor reflexes. *Physiological Reviews* **56**, 100–176.

KRNJEVIC, K., PUIL, E. & WERMAN, R. (1977). GABA and glycine action on spinal motoneurones. *Canadian Journal of Physiology and Pharmacology* **55**, 658–669.

MCLEAN, J. H. & HOPKINS, D. A. (1982). Ultrastructural identification of labeled neurons in the dorsal motor nucleus of the vagus nerve following injections of horseradish peroxidase into the vagus nerve and brainstem. *Journal of Comparative Neurology* **206**, 243–252.

MEI, N., CONDAMIN, M. & BOYER, A. (1980). The composition of the vagus nerve of the cat. *Cell and Tissue Research* **209**, 423–431.

MERRILL, E. G., LIPSKI, J., KUBIN, L. & FEDORKO, L. (1983). Origin of the expiratory inhibition of nucleus tractus solitarius inspiratory neurones. *Brain Research* **263**, 43–50.

MILES, R. (1985). Low frequency depression of synaptic transmission in the nucleus of the solitary tract *in vitro*. In *Neurogenesis of Central Respiratory Rhythm*, ed. BIANCHI, A. L. & DENAVIT-SAUBIÉ, M., pp. 165–168. Lancaster: MTP Press.

MILLER, A. J. (1982). Deglutition. *Physiological Reviews* **62**, 129–186.

MORIN-SURUN, M. P., CHAMPAGNAT, J., BOUDINOT, E. & DENAVIT-SAUBIÉ, M. (1984). Differentiation of two respiratory areas in the cat medulla using kainic acid. *Respiration Physiology* **58**, 323–334.

PAINTAL, A. S. (1973). Vagal sensory receptors and their reflex effects. *Physiological Reviews* **53**, 159–227.

RALL, W., BURKE, R. E., SMITH, T. G., NELSON, P. G. & FRANK, K. (1967). Dendritic location of synapses and possible mechanisms for the monosynaptic epsp in motoneurons. *Journal of Neurophysiology* **30**, 1169–1193.

RICHTER, D. W. (1982). Generation and maintenance of the respiratory rhythm. *Journal of Experimental Biology* **100**, 93–107.

RITCHIE, T. C., WESTLUND, K. N., BOWKER, R. M., COULTER, J. D. & LEONARD, R. B. (1982). The relationship of medullary catecholaminergic containing neurones to the vagal motor nuclei. *Neuroscience* **7**, 1471–1482.

SHAPIRO, R. E. & MISELIS, R. R. (1985). The central organization of the vagus nerve innervating the stomach of the rat. *Journal of Comparative Neurology* **238**, 473–488.

SPYER, K. M. (1982). Central nervous integration of cardiovascular control. *Journal of Experimental Biology* **100**, 109–128.

TAKAGI, H., KUBOTA, Y., MORI, S., TATEISHI, K., HAMAOKA, T. & TOHYAMA, M. (1984). Fine structural studies of cholecystokinin-8-like immunoreactive neurons and axon terminals in the nucleus of tractus solitarius of the rat. *Journal of Comparative Neurology* **227**, 369–379.

URBAN, L. & RANDIC, M. (1984). Slow excitatory transmission in rat dorsal horn: possible mediation by peptides. *Brain Research* **290**, 336–341.

VAN DER KOOY, D., KODA, L. Y., MCGINTY, J. F., GERFEN, C. R. & BLOOM, F. E. (1984). The organization of projections from the cortex, amygdala and hypothalamus to the nucleus of the solitary tract in the rat. *Journal of Comparative Neurology* **224**, 1–24.

VON EULER, C., HAYWARD, J. N., MARTILLA, I. & WYMAN, R. J. (1973). Respiratory neurons of the ventrolateral nucleus of the solitarius vagal input; spinal connections and morphological identification. *Brain Research* **61**, 1–22.

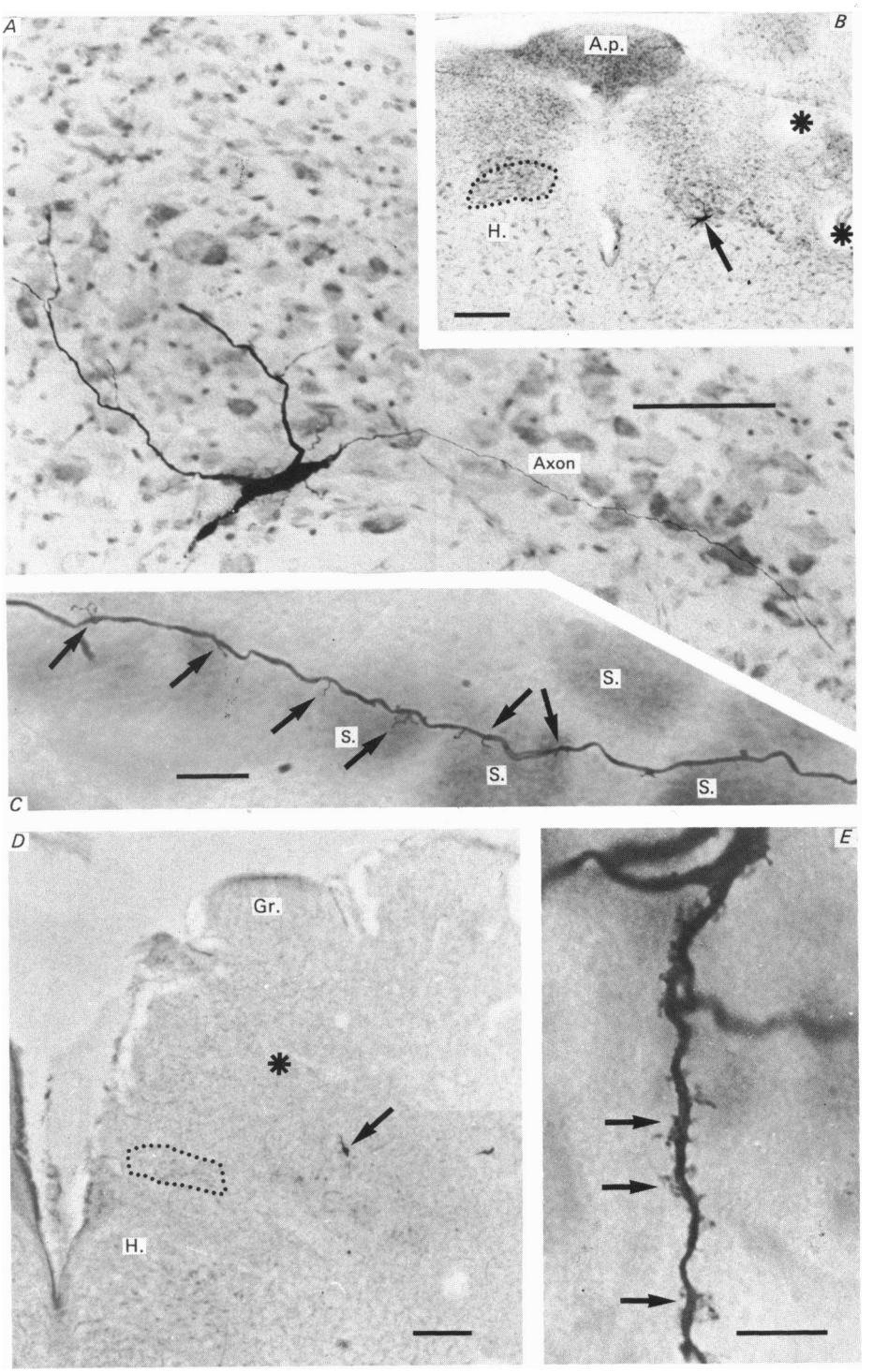

For description of plate see p. 573.

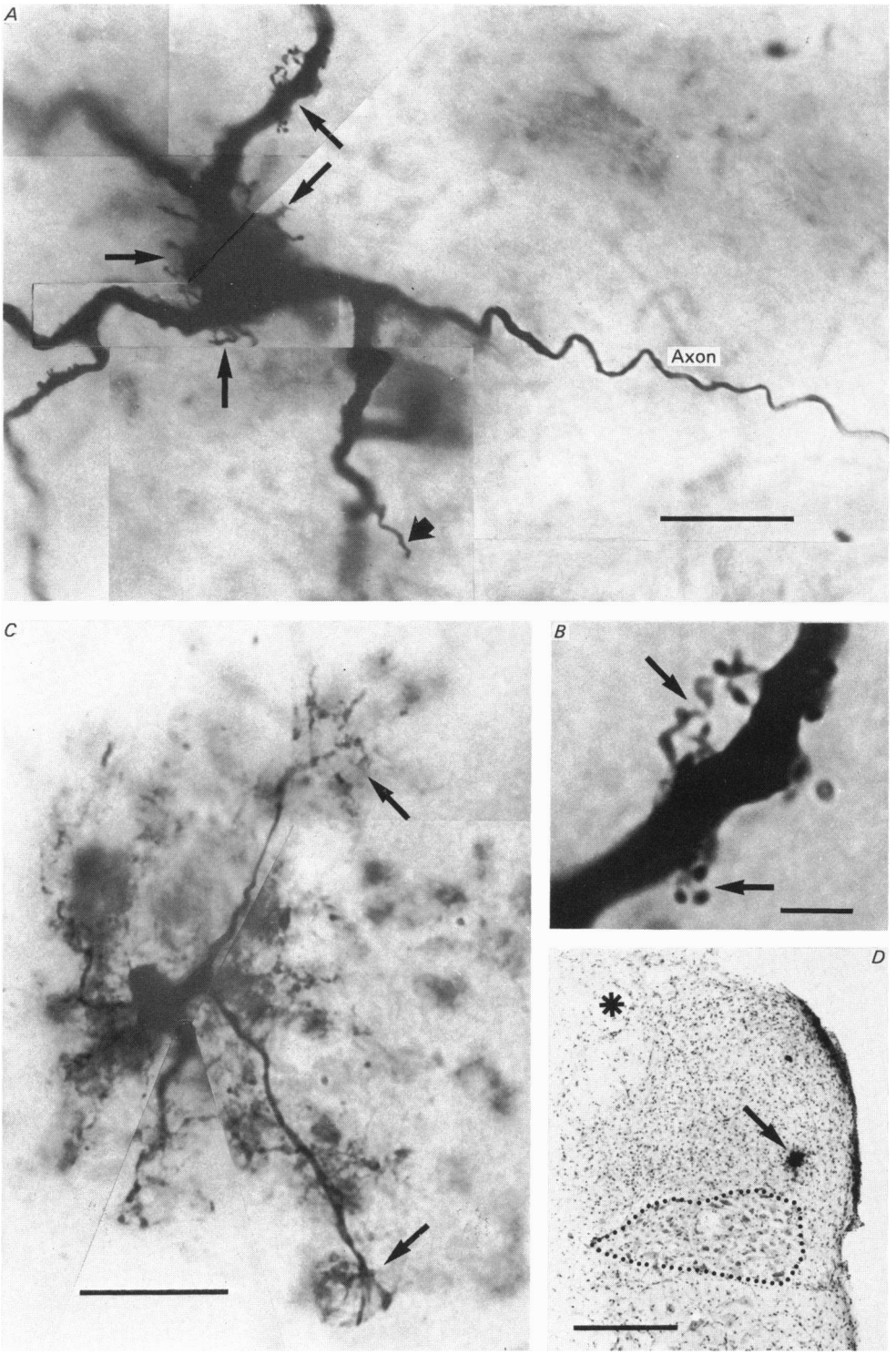
A
Axon
C
B
D

EXPLANATION OF PLATES

PLATE 1

Morphology and anatomical situation of rat d.v.m.n. (*A*, *B* and *C*) and cat ventrolateral nucleus tractus solitarius (*D* and *E*) neurones. In *A*, soma, proximal dendrites and axon; calibration: 100 μm. In *B*, anatomical localization of the same neurone; calibration: 250 μm; the positions of stimulating electrodes are indicated by stars and arrow indicates the cell body of the neurone; the left d.v.m.n. is outlined with dots; a.p., area postrema; h., hypoglossus nucleus. In *C*, axon of the cell illustrated in *A* and *B*; arrows indicate small beaded collaterals; s., soma of neighbouring neurones of the d.v.m.n. In *D*, anatomical location of an horseradish peroxidase-labelled soma (arrow) in the right ventrolateral nucleus tractus solitarius of the cat (neurone reconstructed in Fig. 9); star, localization of the stimulating electrode; the right d.v.m.n. is outlined with dots; gr., nucleus gracilis; h., nucleus hypoglossus; calibration: 250 μm. In *E*, primary dendrite of the neurone illustrated in *D*; calibration: 10 μm; arrows, spiny and filament-like processes.

PLATE 2

Morphology of neurones with p.r.e. (*A* and *B*) and p.i.e. (*C* and *D*) in the rat medial nucleus tractus solitarius. In *A*, soma, proximal dendrite and axon of the neurone reconstructed in Fig. 8. Note a filament-like dendritic spine (large arrow) and beaded spines (small arrows) on soma and dendrites; calibration: 25 μm. In *B*, higher magnification view of beaded dendritic spines from the same neurone; calibration: 5 μm. In *C*, morphology of a neurone with p.i.e.; arrows indicate neurite arborization in the proximity of neighbouring cell bodies; calibration: 20 μm. In *D*, situation (arrow) of the neurone illustrated in *C*; the d.v.m.n. is outlined with dots; star, position of the stimulating electrode.